Interfacial Kinetics of HOR/MOR at the AEM/Pt Microelectrode Interface: Investigation of the Influence of CO_3^{2-} on the Reaction Kinetics and the Mass Transport through Membrane

Iromie Gunasekara, Ian Kendrick, and Sanjeev Mukerjee *,z

Northeastern University Center for Renewable Energy Technology, Department of Chemistry and Chemical Biology, Northeastern University, Boston, Massachusetts 02115, USA

The kinetics of hydrogen oxidation reaction (HOR) and methanol oxidation reaction (MOR) at the Tokuyama anion exchange membrane/ Pt microelectrode interface were investigated using a solid state electrochemical cell. Carbonate ions in the membrane which are strongly adsorbing anions; suppress both HOR and MOR kinetics. Carbonate ions not only have a site blocking effect, but at low pHs sufficient amount of hydroxyl ions are not available for adsorption. Adsorption effects by the quaternary ammonium species in the membrane, on the Pt electrode is found to be minimal. However, an ionomer film (AS4) coated on the membrane, significantly decreased the rate of HOR. Diffusion of hydrogen molecules through the membrane was not influenced by the carbonate ions due to the smaller size of the gaseous molecule. However, hydrogen concentration in the anion exchange membrane is low in the presence of carbonate ions. Methanol diffusion is facilitated in the anion exchange polymer electrolyte due to its high water content. However, change of the diffusion path length in carbonate polymer electrolytes caused methanol permeability to drop significantly.
 [DOI: 10.1149/2.0011913jes]

Manuscript submitted May 15, 2019; revised manuscript received July 17, 2019. Published August 9, 2019.

Fuel cells are amongst the important renewable energy sources of interest pertaining to the high demand of portable power. Development of alkaline membrane fuel cells involves addressing problems related to both anode (hydrogen/methanol oxidation) and cathode (oxygen reduction) reactions.[2] Comprehensive characterization of the reactions at the membrane-electrode interface will aid the development of new electro-catalysts, membranes and the optimization of cell design. Electrochemistry at the platinum catalyst-polymer electrolyte interface has been widely studied by measuring the reaction currents by rotating disc electrodes as well as by in-situ fuel cell experiments.[3] State of art H_2/O_2 fuel cells using proton exchange membranes (PEM) have shown 700 mW cm^{-2} power densities at 0.65 V (anode and cathode loading of 0.4 mg_{Pt} cm^{-2}). Despite the generous amount of platinum used, direct alcohol fuel cells (DAFCs) working under acidic environments can only go up to 8 mW cm^{-2} at 0.5V.[4]

To address the issue of reducing the platinum metal consumption in PEM fuel cell electrodes, current research is moving toward using non-platinum group catalysts. In acidic media, these catalysts oxidize at under normal fuel cell operating conditions, and therefore require alkaline environments for use in this context.[5–7] In addition to the feasibility of the oxygen reduction reaction on non-PGM cathodes under low pHs, the possibility to address the water management issues in traditional PEM fuel cells has led to the rapid popularity of this area of research.[8,9]

Polarization losses observed for the anode reaction (hydrogen oxidation) are very low in acidic electrolytes, in fact lowering of platinum loading from 0.4mg cm^{-2} to 0.05mg cm^{-2} has not resulted in a considerable over-potential loss according to in-situ experiments reported by Gastiger et al.[10] However hydrogen oxidation reaction (HOR)/hydrogen evolution reaction (HER) over-potentials are significantly high in alkaline environments.[11]

Hydrogen oxidation and evolution reaction.—One of the primary purposes of this study is to elucidate the mechanism of HOR/HER at the Pt/AEM interface. Much work has been done to study these reactions on Rotating Disc Electrodes (RDE) in both acidic and alkaline aqueous solutions.[1,12,13] HOR/HER on platinum electrodes can take place through the following steps (Equations 1–3),

$$H_2 + 2Pt \rightarrow 2\,(Pt - H) \qquad \text{Tafel} \qquad [1]$$

$$H_2 + Pt \rightarrow Pt - H + H^+ + e \qquad \text{Heyrowsky} \qquad [2]$$

$$Pt - H \rightarrow H^+ + e \qquad \text{Volmer} \qquad [3]$$

Corresponding reactions for an alkaline electrolyte are given by Equations 4–5.

$$H_2 + OH^- + Pt \rightarrow Pt - H + H_2O + e \qquad \text{Heyrowsky} \qquad [4]$$

$$Pt - H + OH^- \rightarrow H_2O + e \qquad \text{Volmer} \qquad [5]$$

HER/HOR in acidic medium is extremely difficult to study as the kinetic region overlaps with the diffusion over-potential region.[1] Various studies have been carried out using acidic electrolytes on Pt(*hkl*) surfaces over the decades and a wide range of exchange current densities have been reported.[12,14,15] HER/ HOR exchange currents reported for alkaline electrolytes are slightly (one order of magnitude) lower than that in acidic medium (~1 mA cm^{-2}).[1] Studies of low index Pt single crystal surfaces in sulfuric acid has revealed HOR reaction rates in the increasing order of Pt (111) < (100) < (110);[14,16] with the rate on (110) being three times than that of (111). Markovic et al. has proposed that the Tafel-Volmer mechanism dominates on Pt(*hkl*) in acidic medium; Tafel step being the rds. The trend observed for alkaline solutions showed similar activity at Pt (111), (100) surfaces and Pt(110) surface showed highest activity.[14]

Similarly, the rate of HER is reported to be significantly lower in alkaline environments than in acidic environments. In alkaline electrolytes, the H^+ atom required in the reaction is abstracted from a water molecule whereas in acidic solutions H^+ is provided by a hydronium ions present. Similar structure sensitivity has been observed for hydrogen evolution in both acidic and alkaline environments where the reaction rates showed an increasing order of Pt(100)<(111)< (110).[17] Sweeping the potential toward negative potentials from the reversible potential, the Pt surface is covered with under-potential deposited hydrogen (H_{upd}) which is a strongly bound species. H_{upd} are not believed to be reactive intermediates for the reaction. Reactive intermediates or weakly bound hydrogen (H_{ad}) are adsorbed at slightly higher over-potentials, with H_{upd} or on top of the H_{upd} layer. These different rates of HOR on different planes mainly arise from the structure sensitivity of the H_{upd} and OH_{ad} formation.[11] At low over-potentials HOR is determined by the coverage of the H_{upd} whereas at higher potentials the role of adsorbed OH comes in to play. Rather than a mere site blocking agent, Conway et al. has considered H_{upd} as a species which influences the H_{ad} bond energy.[18] DFT calculations as well as experimental observations support *Heyrowski –Volmer* mechanism for HOR/HER in aqueous alkaline solutions.[1,19] Pt–H bond distances obtained by theoretical calculations have shown that the transition state bond lengths are low for alkaline solution.[20,21] High OH_{ad} coverage

*Electrochemical Society Fellow.
zE-mail: s.mukerjee@neu.edu

on platinum metal surfaces in alkaline solutions as well as strong Pt-H bonds are responsible for the observed lower exchange currents compared to the acidic environments. No significant effect on Pt particle size was observed.[1] Therefore the HOR/HER mechanism on AEM/Pt(pc) surfaces can be thought to represent the actual mechanism that takes place at a fuel cell anode.

Methanol oxidation reaction (MOR).—Oxidation of methanol on platinum surfaces has been studied extensively over the years.[5,17,22–24] The major concern regarding the use of methanol in fuel cells is the self-poisoning of the platinum surface by MOR products.[25] The MOR mechanism has been studied on polycrystalline Pt,[26–28] single crystal Pt[5,17,22,24] surfaces as well as on Pt-alloy[23,29,30] catalysts. Methanol oxidation in alkaline environments proceeds faster than that in acidic electrolytes. The inability of platinum metal sites to adsorb sufficient amount of hydroxyl species is the reason behind the slower kinetics observed in low pHs.[28] On the other hand, balanced co-adsorption of hydroxyl species in high pHs facilitates the reaction. However MOR kinetics is influenced by the progressive production of CO_2 species as an end product which reduces the pH of the alkaline electrolyte. MOR has been extensively studied by Tripkovic et al.[5,17,24] on low index platinum single crystals. The two-way mechanism which has been proposed for MOR is shown by Equation 6.

$$CH_3OH \rightarrow Reactive\ intermediates \begin{matrix} \nearrow HCOO^- \\ \searrow Poisoning\ species \rightarrow CO_2 \end{matrix} \quad [6]$$

Formates are produced from HCO_{ad} reactive intermediate and CO_2 from the strongly bound CO. FT-IR measurements have shown that the main poison on the platinum electrode is CO species.[5] Poisoning of the Pt surface by CO is dependent on the Pt crystal plane where the Pt(111) plane is more prone to CO poisoning.[17] Part of the CO_{ad} species will be oxidized to carbon dioxide by oxygen containing species adsorbed on to the metal surface. Addition of metals such as ruthenium has been effective for its high hydrophilic nature. Gastiger et al. has proposed that the optimum amount of Ru in Pt to be 10% atomic ratio.[31] However, Tripkovic et al. reported similar kinetics for methanol oxidation on Pt and Pt_2Ru_3 catalysts.[23]

Alkaline anion exchange membrane carbonate ion enrichment.—The major challenge when dealing with alkaline environments is the reaction of OH^- ions with atmospheric carbon dioxide leading to a mixture of carbonate/bicarbonate in the membrane.[2,23,32] There is a controversy about the exact composition of anion inside the membrane. However, reports suggest that carbonate ion enrichment is feasible in fuel cell operating conditions. Selectivity of AEMs for carbonate ions is explained by the Donnan exclusion effect where the H^+ ions are excluded from the membranes.[33] Prior reports have shown that the pore solution pH increases hence becomes rich in multi charged anions.[34–37]

For a H_2/Air fuel cell under operation, current density determines the carbonate ion concentration inside the membrane. Towards higher current densities, the anion composition inside the AEM becomes a mixture of only carbonate/hydroxide ions due to the progressive production of hydroxide ions at the cathode.[38] Detection of carbon dioxide in the anode exhaust in such conditions further suggests the presence of carbonate ions as charge carriers and supports Equation 7 over Equation 8 as the anode reaction.

$$H_2 + CO_3^{2-} \rightarrow CO_2 + H_2O + 2e \quad [7]$$

$$H_2 + CO_3^{2-} \rightarrow 2HCO_3^- + 2e \quad [8]$$

Further, Equation 9 is rationalized for the anode reaction for Methanol/Air AEM fuel cells.[39]

$$CH_3OH + 3CO_3^{2-} \rightarrow 4CO_2 + 2H_2O + 6e \quad [9]$$

Therefore, the popular argument that the low performances observed in H_2/air alkaline fuel cells are due to the bicarbonate ions, can be ruled out. In this study, a Pt working electrode and an AEM in carbonate ion phase was used to represent a fuel cell anode operating under atmospheric air feed. The experimental observations of Lang et al.[39] further suggest that methanol/air fuel cell membrane will be enriched in carbonate ions over bicarbonate ions (Equation 9).

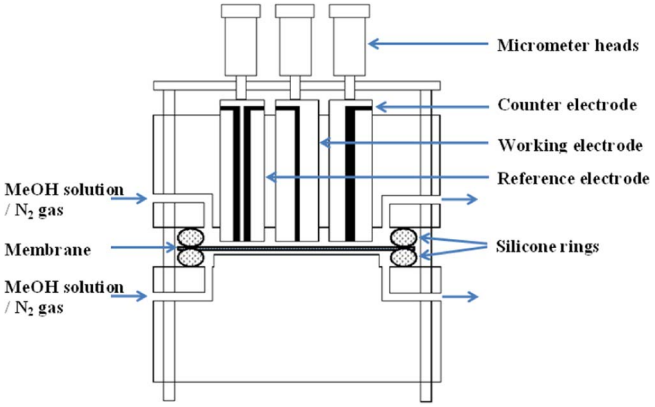

Figure A. Liquid feed enabled solid state cell.

Microelectrode investigations of hydrogen/methanol oxidation reactions.—As an attempt to mimic the membrane-electrode interface in a fuel cell, hydrogen oxidation and methanol oxidation reactions have been studied on Pt microelectrode/ PEM interface.[27,40–42] In our study, anion exchange membranes Tokuyama A201 and A901 (28 μm and 10 μm thick, respectively) were used in a solid-state half-cell configuration[43,44] employing a Pt micro-disc electrode. The importance of the microelectrode with regard to solid polymer electrolytes is the improved mass transport on to the electrode surface with no need of an external (hydrodynamic) force as in RDE. Furthermore, due to the insignificant *iR* losses in relation with the low currents at micro-disc electrodes, a supporting electrolyte is not required, thereby eliminating undesirable anion adsorption. In previous microelectrode characterization attempts of the Pt/Nafion interface, reduced anion adsorption due to absence of a supporting electrolyte has been beneficial to the reaction kinetics.[40] Tafel slopes of 29 mV dec^{-1} have been reported for HOR and hydrogen transport through the membrane similar to that observed in aqueous acidic electrolytes. Similarly, detailed studies on the methanol oxidation mechanism at an acidic polymer electrolyte have been reported. According to Kucernack et al.[27] even in the absence of solid polymer, Pt sites are accessible to the intermediate reactants through surface diffusion.

Our previous work[37] reports a detailed study of oxygen reduction electrochemistry at the AEM-electrode interface under controlled atmospheric conditions. Here we suggest that fuel cell anode reactions (hydrogen/methanol oxidation) have significant effects imposed by the carbonate ions introduced to the AEM. In addition to that, anion adsorption on the platinum surface by the soluble ionomer present at the interface is discussed. Our prior publication[45] reported that quaternary ammonium ions present in small molecules specifically adsorb on to the electrode surface and unsuitable double layer effects are induced. Here we use the advantage of the solid state electrochemical cell to further support that argument.

Experimental

Membranes and electrodes.—Tokuyama-A201(OH) and A901(OH) (Tokuyama Corp., Tsukuba, Japan) membranes were pretreated by soaking the membranes in 1M KOH solutions. Membranes were then rinsed and stored in CO_2 free water. Membranes in the carbonate form were prepared by soaking as received membranes in 1M K_2CO_3 solution. These membranes were then rinsed and stored in milli-q water overnight to leach excess carbonate ions. A solid state cell as discussed in our previous publications was used for HOR studies.[37,43,44] Liquid feed enabled cell shown in Figure A was used for MOR studies. 100μm Pt microelectrode (Bio-analytical systems),

1.6 mm diameter Pt disc counter electrode and a dynamic hydrogen electrode (DHE) made the three electrode system. All electrodes were cleaned using 15μm, 3μm, 1μm diamond polish respectively and were sonicated in milli-q water for 10 minutes.

Electrochemical analysis.—Electrochemical measurements were recorded using a computer controlled potentiostat/galvanostat (Autolab, model PGSTAT 30) at room temperature and 1 atm pressure. Measurements for AEM(OH) were performed in an Atmos-glove bag (Sigma Aldrich) to create a CO_2 free environment. Cyclic voltammograms were recorded for 100%RH nitrogen saturated membranes to ensure proper electrochemical interface. Cyclic voltammograms for hydrogen saturated membranes were recorded at 2 mVs^{-1}.

Using the mathematical model proposed by Aoki and Osteryoung[46] to simulate chronoamperometric currents at the microelectrode, Winlove et al.[47] have reported that if the time after polarization is small, diffusion limited current at the microelectrode can be given by modified Cottrell equation (Equation 10).

$$I = \frac{nFAD^{\frac{1}{2}}C}{\pi^{\frac{1}{2}}t^{\frac{1}{2}}} + n\pi FDCr \qquad [10]$$

Chronoamperometric measurements were carried out by equilibrating the electrode at potential close to the open circuit potential and stepping up to a potential beyond the kinetic region. Contact impedance was measured using FRA spectroscopy and the built in micrometer heads were adjusted until the contact pressure was minimum.[37] The active surface area of the microelectrode was determined by the integration of the H_{upd} area measured by the voltammogram. D and C were calculated by using the equations involving the slope and the intercept of the Cottrell plot.[37,48]

$$D = \frac{intercept^2 \times r^2}{slope^2 \times \pi}, \qquad [11]$$

$$C = \frac{slope^2}{intercept \times r^3 \times F \times n} \qquad [12]$$

To interpret Heyrowky-Volmer reaction with a transfer coefficient of α, the Butler –Volmer(B-V) equation can be used.[1] Kinetic parameters for HOR were obtained by fitting the polarization data in B-V equation[1] (Equation 13).

$$i_k = i_o \left\{ \exp\left(\frac{\alpha F}{RT}\eta\right) - \exp\left(\frac{-(1-\alpha)F}{RT}\right)\eta \right\} \qquad [13]$$

Current densities are corrected for mass transport limitation using Equation 14 prior to being fitted to the Butler-Volmer equation.

$$\frac{1}{i_k} = \frac{1}{i_{meas}} - \frac{1}{i_{lim}} \qquad [14]$$

Results and Discussion

In order to optimize the contact between the membrane and the electrode, and to clarify the proper electrochemical interface, cyclic voltammograms were recorded for the nitrogen saturated alkaline membrane (Figure 1). All the potentials reported here are corrected to the standard hydrogen electrode scale using the hydrogen evolution potential. Figure 1 shows the required features for a cyclic voltammogram recorded in nitrogen saturated alkaline electrolyte under 100% RH conditions. We were able to calculate the electrochemically active area of the electrode using the hydrogen adsorption region of the nitrogen cyclic voltammogram. The potential from 0.05 V to 0.4 V shows the hydrogen adsorption region.

The peak appearing at the 0.6 V to 0.85 V regions is the hydroxide adsorption region. Cyclic voltammograms reported for Pt/PEM interfaces have shown that the hydroxide adsorption commences at lower potentials than that observed in aqueous H_2SO_4 solutions due to reduced anion adsorption in polymer electrolyte interface.[40] The OH_{ad} formation charge in aqueous NaOH vs. aqueous $HClO_4$ solutions are reported to be significantly different.[49] According to Figure 1, similar

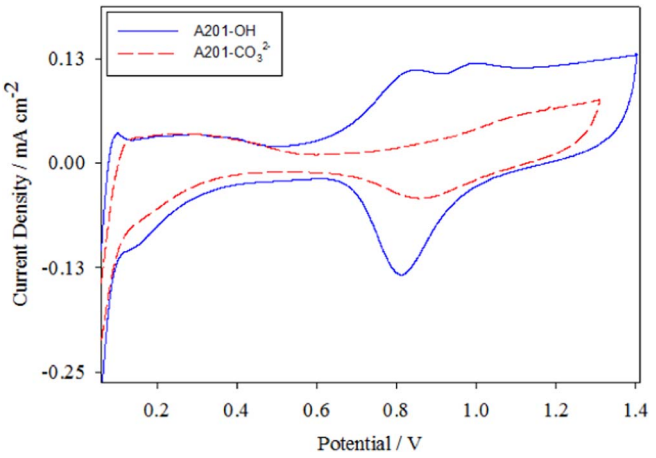

Figure 1. Cyclic voltammogram recorded on A201 membrane under 100% RH nitrogen saturated conditions, 293K, 1 atm.

potential behavior is observed for Pt/AEM interface as that in aqueous NaOH solutions. This behavior is expected as there are no adsorbing anions present in those two solutions other than the hydroxide ions. It is clearly seen that the hydroxide adsorption region is shifted toward positive potentials in the CO_3^{2-} electrolyte, and at the same time the peak is suppressed in carbonate electrolytes. In the Nafion/Pt membrane, the potential of OH_{ad} formation has been shifted to lower potentials than that observed in aqueous sulfuric acid conditions.[40] This observation is in agreement with the carbonate (anion) adsorption on the Pt surface. Carbonate ions impose a strong adsorbing effect on the Pt surface. The butterfly peak mainly arises from OH adsorption. Therefore, the decrease in formation charge (peak area) is expected for carbonate polymer electrolytes.

Hydrogen oxidation kinetics.—Inset of Figure 2A shows HOR/HER polarization curves at the AEM/Pt(hkl) interface. The blue curve represents the membrane in the hydroxide form while the curve in red represents the membrane in the carbonate form. IR correction applied to the I-V curves did not make a significant difference due to the currents in the order of ∼nA magnitude recorded. Hydrogen oxidation current reaches its limiting region after a potential of 0.2V.

The limiting current of 0.16 mA cm^{-2} for the A201(OH) membrane decreases to 0.05mA cm^{-2} upon exchange of the membrane to carbonate form. Figure 2A shows the mass transport corrected Tafel plots for the two types of membranes of interest. HOR exchange current density for the membrane in the hydroxide form, 0.63mA cm^{-2} is in good agreement with 0.69mA cm^{-2}, the value reported for a 0.1 M aqueous KOH solution by Gastiger et al.[1] HOR current densities were obtained by fitting the Tafel plot in the region between 0V and 0.1V in the Butler-volmer (Equation 13, Table I). The transfer coefficient of 0.48 well agrees with the Heyrowski-Volmer mechanism proposed by DFT calculations.[19] The decreased HOR exchange current is in agreement with the decreased surface activity observed in carbonate solutions.[5] The symmetry of the Tafel plot obtained for A201(OH) suggests a similar mechanism for HER on the Pt/microelectrode interface.[1]

Table I. Kinetic parameters for hydrogen oxidation reaction.

Electrolyte	j_o (mA/cm^{-2})	Tranfer coefficient - α
0.1 M KOH[1]	0.69	0.50
AEM (OH^-)	0.63	0.48
AEM (CO_3^{2-})	0.09	0.88
AEM(OH)+AS4	0.05	0.50

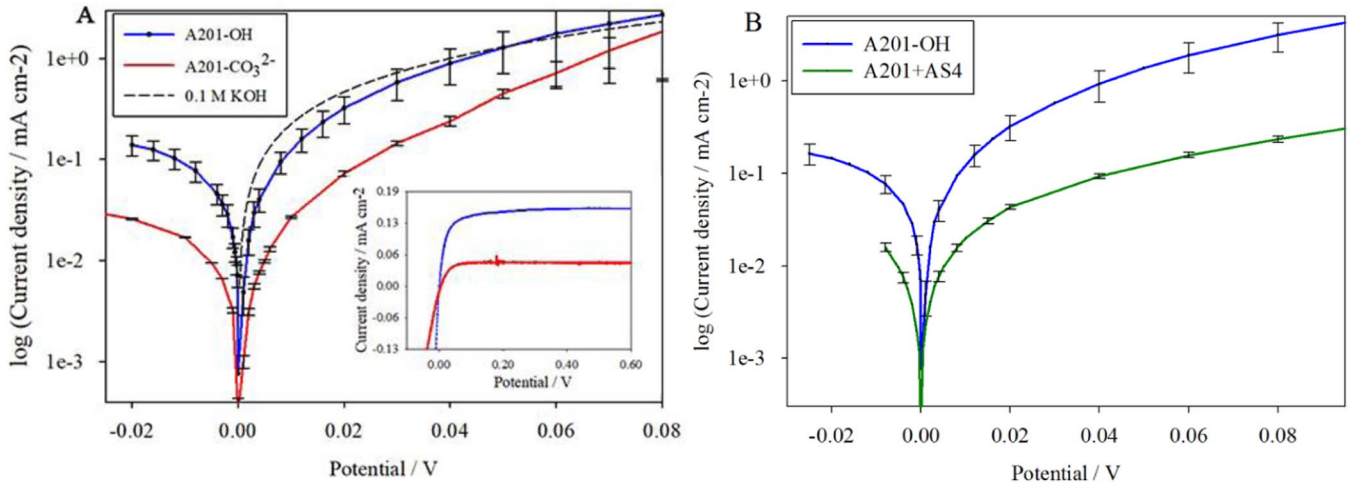

Figure 2. Mass transport corrected Tafel plots for HOR/HER at the membrane electrode interface. A: Comparison of A201(OH) with A201(CO_3^{2-}). B: Kinetics in the presence of 0.4mgcm^{-2} AS4 coating on the membrane.

HOR in the presence of AS4 ionomer film.—Figure 2B compares the kinetic currents at a Pt microelectrode/A201(OH) membrane interface with and without a coating of 0.4 mg cm^{-2} AS4 ionomer. It is quite interesting that the kinetic current in a 0.1 M KOH solution is not much different from the kinetic current observed at the A201(OH) membrane/electrode interface whereas in the presence of an ionomer coating, the current has significantly decreased (Figure 2B). A similar observation has been made by Unlu et al. for the methanol oxidation reaction (MOR) in the presence of tetra-methyl ammonium hydroxide (TMA^+OH^-) and TMA^+ tethered polymer (PTMAOH).[45]

Depending on the length of the side chain and the size of the alkyl substituent on the nitrogen atom an ionomer can form a compact double layer structure at the electrode, leading to slow HOR kinetics.

Hydrogen mass transport.—Transport of gaseous molecules through the membrane is determined by their solubility in the membrane and their diffusion. The mass transport data shown in Table II was derived from the Cottrell plots shown in Figure 3. Hydrogen solubility in water is in the order of $\sim 10^{-7}$ mol cm^{-3}. Ion exchange capacity of a given membrane is related to its equivalent weight and it gives an insight to the side chain length of the membrane (high ion exchange capacity of AEMs correlated with low side chain length). The low diffusion of hydrogen molecules in AEM regardless of the high water content (or IEC) implies that the hydrogen molecule diffusion does not take place through the aqueous part of the polymer membrane. In a study on Nafion membranes, Tsuo et al.[50] concluded that since the solubility of hydrogen in proton exchange membranes is lower than of water, yet higher than that of polytetrafluorinated ethylene, the of extrusion of side chains to the water phase is an important factor for determining the diffusion path of hydrogen molecules. A similar rationale can be applied in the context of A201/A209: since the solubility of hydrogen in AEMs falls between water and polystyrene, it is reasonable to believe that the hydrogen molecules dissolve and diffuse through the water polymer interfacial regions of the membrane.[50,51]

Table II. Mass transport characteristics of Hydrogen in the AEM.

Electrolyte	Diffusion coefficient $D10^6$ ($cm^2\ s^{-1}$)	Solubility $C10^6$ (mol cm^{-3})	Permeability $DC10^{12}$ (mol $cm^{-1}\ s^{-1}$)
AAEM-(OH^-)	1.34	2.98	4.00
AAEM-(CO_3^{2-})	1.30	0.52	0.68
Nafion 117	7.60	0.51	3.90

The crystallinity of the water phase decreases with the increase of the water content whereby the extrusion of the hydrophobic phase in to the water phase increases. This in turn increases the interfacial path length, decreasing the overall H_2 diffusion coefficient. It is interesting that D_{H2} is not altered when the mobile ion is changed from OH^- to CO_3^{2-}. This also is an indication that the hydrogen molecules are indeed diffusing through the interfacial region of the membrane. Ionic species are generally confined to the aqueous part of the membrane, hence has a little effect on molecule transport that occurs through the interfacial region. This will be discussed more in the section of methanol transport through the membrane. The effect of carbonate ions on the hydrogen solubility is not clear.

Methanol oxidation reaction.—Cyclic voltammograms obtained for MOR at different AEM/Pt interfaces are shown in Figure 4. The CV corresponding to the Nafion/Pt interface is super-imposed in black dashed curves in the same figure for better clarity. MOR begins at a potential of 0.5V, after the hydrogen desorption region. Voltammograms shown in Figure 4 indicate that the methanol oxidation peak current coincides with the hydroxide layer formation.[5,17,22,24] At potentials above 0.9V, the electrode surface becomes highly covered by hydroxyl species which inhibits MOR. The CVs clearly show the

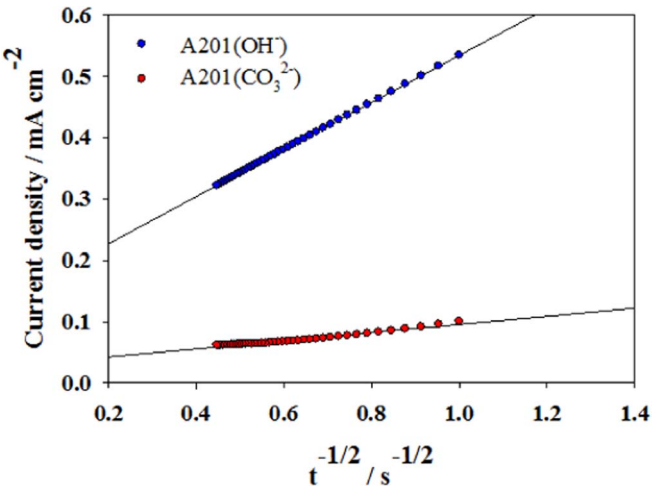

Figure 3. Cottrell plots for the HOR calculated from current-time transients at 0.3V (potential jump from 0V to 0.3 V.

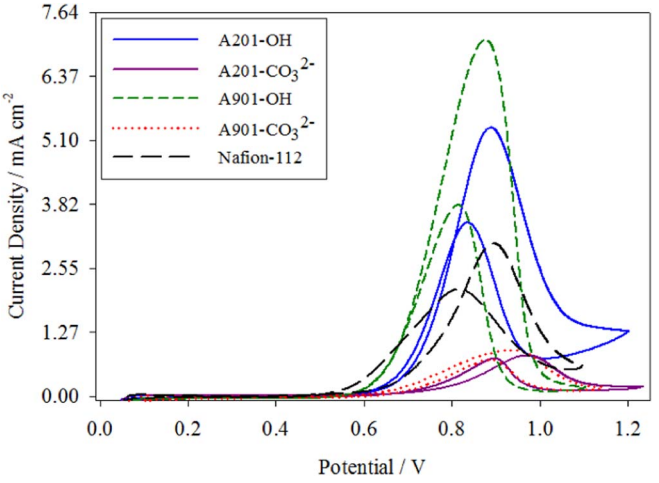

Figure 4. Cyclic voltammograms for MOR at the membrane/Pt microelectrode interface. 1 M MeOH, 293K.

low onset potentials for MOR at A201(OH) and A901(OH) interfaces compared to MOR at Nafion membrane.

The decrease in reverse peak current is due to CO poisoning species formed when the MOR progresses. Reverse peak at the Nafion membrane interface appears at much lower potentials than the forward peak. In alkaline electrolytes the electrode surface recovers more easily therefore a shift in reverse peak is not observed. When comparing the effect of the carbonate ion on the reaction, the effect of anionic adsorption on MOR needs to be taken into consideration. Effect of anionic species has been extensively studied in both acid and alkaline aqueous electrolytes. In a study involving electrolytes with HSO_4^-, $HClO_4^-$ and $H_2PO_4^-$ anions, Wieckowski et al.[22] have reported that the rate of the reaction is highly dependent on the relative strength of a particular anion to adsorb on to the electrode surface. Methanol oxidation reaction is found to be highly dependent on the pH of the solution.[23] Low activity of Pt surfaces for MOR in carbonate electrolytes can be explained as follows: Carbonate ions in the AEM influence OH adsorption on Pt(hkl) surfaces. Adsorption of carbonate ions on the metal surface reduces the coverage of methanol as well as OH_{ad}. In alkaline electrolytes, it has been shown that MOR commences at 0.4 V in NaOH, $NaHCO_3$ and Na_2CO_3.[23,24,49] However, the initial surface activity decreases in the order of $OH > CO_3^{2-} > HCO_3^-$.

Table III. Kinetic parameters for Methanol oxidation reaction.

Electrolyte	Tafel Slope mV dec^{-1}	j at 0.65 V 10^{-5} A cm^{-2}
A201(OH)	142	4.32
A201(CO_3^{2-})	314	1.00
A901(OH)	122	15.06
A901(CO_3^{2-})	249	1.00
0.1M OH solution	121	294.4
Nafion 112	138	4.12

Tripkovic et al.[24] has reported that in aqueous alkaline solutions, electro-sorption of hydroxide ions are coupled with bicarbonate and carbonate ions in corresponding anion solutions. In addition, adsorbed carbonate ions on the electrode surface shift the onset potential of MOR. CVs obtained for N_2 saturated membranes (Figure 1) shows that adsorption of carbonate ions cause a positive shift in the OH_{ad} formation region. The surface activity is determined by θ_{OH} therefore, decrease in peak currents are expected in carbonate electrolytes. In Figure 4 we have observed a depression of peak currents as expected. However, compared to that reported for aqueous electrolytes the differences observed here are large.[5,17,24] This fact may be coupled with the mass transport complications in solid polymer electrolytes, which needs more investigation.

Methanol oxidation kinetics.—Figure 5A compares the activity in hydroxide and carbonate forms of A-201 membrane with that of Nafion 112 and aqueous KOH solution (0.1M). These curves were fitted with Tafel equations with slopes of 142 mV dec^{-1} and 314 mV dec^{-1} for A201(OH) and A201(CO_3^{2-}), respectively. Figure 5B compares the activity in the hydroxide and carbonate forms of A-901 membrane. Higher kinetic currents than that for the A201(OH) were observed for the A901(OH) membrane can be attributed to different surface concentrations of charged sites. Calculated Tafel parameters for these membranes are listed in Table III.

MOR in 0.1 M KOH solution yielded a Tafel slope of 113 which is in agreement with the typical value observed for MOR in alkaline solutions. Kinetic parameters obtained for the interface of the hydroxide form of both A201 and A901 membranes were only slightly lower than that of an aqueous KOH solution. However, the fact that the Tafel

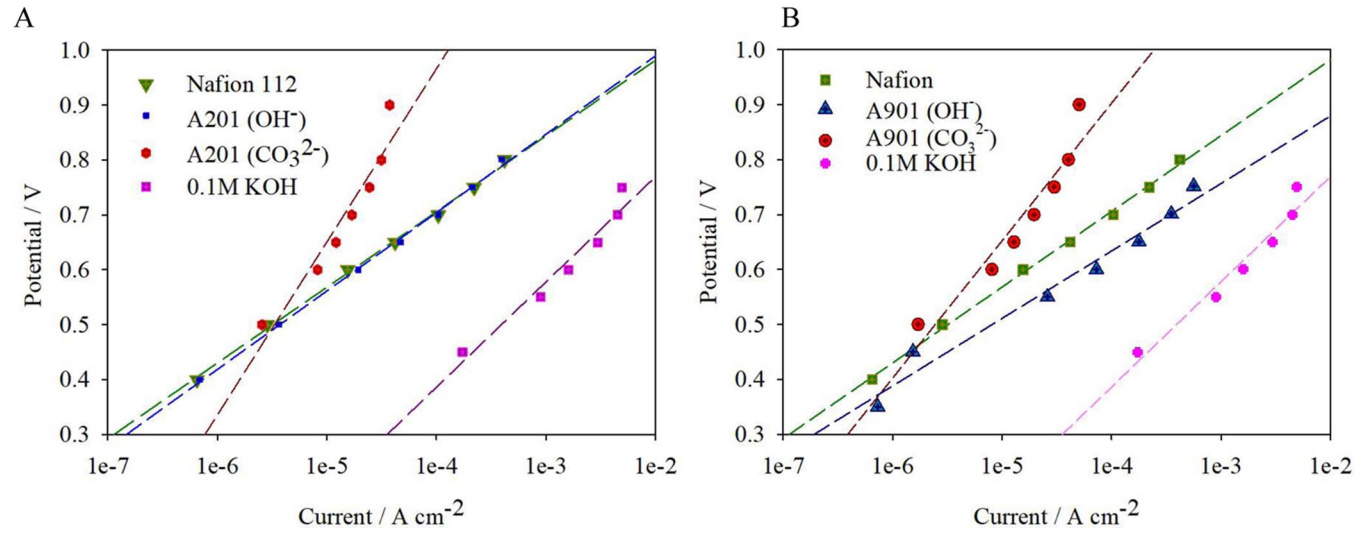

Figure 5. A: Comparison of kinetic parameters for MOR at the Pt/A201 interface, 293K, 1M MeOH - Mass transport corrected Tafel plots, B: Comparison of kinetic parameters for MOR at the Pt/A901 interface, 293K, 1M MeOH.

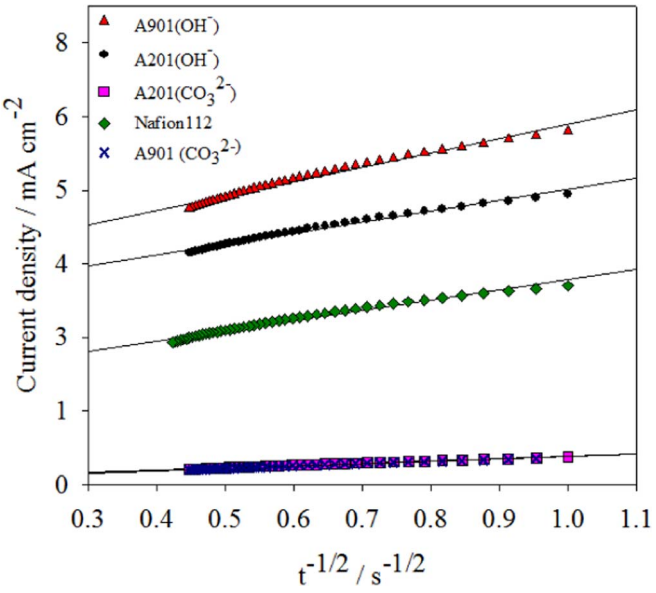

Figure 6. Cottrell plots for the MOR calculated from current-time transients at 0.8V (potential jump from 0.4V to 0.8 V).

slopes change with the pH arises the question if the rate determining step has changed in carbonate solutions. Tafel slopes reported for both hydroxide and carbonate aqueous solutions by Tripkovic et al. were similar in value.[17] It seems that MOR occurs at a slightly modified electrode surface in the carbonate polymer electrolyte. Adsorbed carbonate ions on the Pt surface at the methanol oxidation potentials clearly imposes site blocking effect for adsorption of methanol molecules. The change in MOR Tafel slopes can be further attributed to complicated mass transport related to solid polymer electrolyte interfaces.

Methanol mass transport in the membrane.—Methanol permeation from the anode to the cathode through the membrane is known as methanol crossover in DMFCs. Besides the progressive carbonation of the electrolyte and CO poisoning in the platinum sites, methanol crossover is known as the major problem which causes voltage loss: permeated methanol reacts with oxygen at the cathode to create a mixed potential. The complete (6e) reaction in an alkaline DMFC is shown by Equation 15.

$$CH_3OH + OH^- \rightarrow CO_2 + 4H_2O + 6e \qquad [15]$$

Typically, improved mass transport of the reactants to the electrodes should result in better performance of the cell. However due to crossover of reactants, mass transport through a cell should be taken into consideration. Developing membranes with both high ionic conductivity and low methanol crossover has become a challenge in the field of DMFCs. Ex-situ methanol permeability of membranes would be a measure of how the membrane is resistant to methanol crossover.

Potential step chrono-amperometric measurements were recorded for MOR at the membrane-electrode interface and the Cottrell plots calculated using current time transient are shown in Figure 6. Diffusion and solubility parameters of methanol in membranes obtained using the slope and the intercept of the Cottrell plots (Table IV). Membranes were equilibrated with a 1M methanol solution prior to taking readings. Therefore, methanol flow in and out of the solid state cell does not have a significant effect on the local methanol concentration in the membrane.[27]

Methanol sorption in the membrane.—Studies of methanol uptake by Nafion membranes[52,53] have shown that they do not have a preference for either methanol or water molecules, when the membranes

Table IV. Mass transport characteristics of Methanol in the AEM.

Electrolyte	Diffusion coefficient $D10^6$ ($cm^2\ s^{-1}$)	Solubility $C10^6$ (mol cm^{-3})	Permeability $DC10^{12}$ (mol $cm^{-1}\ s^{-1}$)
A201-(OH^-)	22.4	1.19	26.7
A201- (CO_3^{2-})	0.61	1.22	0.74
A901- (OH^-)	17.0	1.81	30.8
A901- (CO_3^{2-})	0.41	1.93	0.79
Nafion 112	8.0	1.92	15.4

are equilibrated with solutions composed of different concentrations of methanol and water. Chemical polarity of solvents determines the sorption of the molecules withwater sorption being proportional to the ion exchange capacity (or the number of ionic sites) of a particular membrane due to their high polarity. However, methanol molecules would also interact with the hydrophobic region of the membrane. Size of the different molecules should also be taken into consideration. High ionic capacity of AEMs studied predicts a higher affinity for water sorption. The amount of water in the membrane has two effects in the membrane: the absorbed water swells the membrane and increases the ionic cluster size. Enlargement of the water channels facilitates methanol diffusion through the membrane. Table IV shows the calculated methanol permeability values of the membranes investigated. Permeability or crossover of methanol in alkaline DMFCs is determined by several factors. Electro-osmotic drag of the species travelling in the same direction of methanol crossover in cation exchange membranes contributes to high cross over currents. However, in DMAFCs, methanol crossover is in the opposite direction to that of ion transport. This factor leads to low overall methanol permeability. We were able to calculate the methanol permeability of the membrane without electro-osmotic drag contribution. Since the ion exchange capacity of the membrane is not influenced by the carbonate exchange we cannot expect the water content of the carbonated membrane to change significantly. However, the huge drop in diffusion coefficient results in an overall low permeability value. As we have discussed in the section of hydrogen mass transport, the strong ion pairing of quaternary ammonium cationic sites with the doubly charged carbonate species creates a methanol diffusion path around the bulky ion pairs. Increase in path length seems to be the reason behind the overall decrease of methanol molecule diffusion coefficient. The influence of the carbonate ion on the mass transport of methanol however, needs more investigation.

Conclusions

We have successfully employed a solid state electrochemical cell employing a Pt microelectrode to quantify the hydrogen and methanol transport parameters and the interfacial kinetics in alkaline anion exchange membranes. The presence of carbonate ions (in the aqueous region of the membrane) did not affect the D_{H2}, as the hydrogen diffusion took place mainly through the hydrophobic interfacial region. However, hydrogen solubility was greatly reduced. Adsorption of carbonate ions on the Pt(pc) surface at potentials close to the HOR potentials resulted in small exchange current densities in the AEM(CO_3^{2-}). Methanol transport in AEM(OH^-) is better compared to that in proton exchange membranes, as the high water content in AEMs increases the pore sizes and hence facilitates diffusion of molecules in aqueous region. Decreased methanol diffusion in the anion exchange membrane in the carbonate form is explained by the strong ion pairing between the doubly charged carbonate ions with the quaternary ammonium species causing methanol molecules to diffuse around the bulky ion pairs (increasing diffusion path length). Similar to that for HOR, Methanol oxidation kinetics were greatly reduced by the presence of carbonate ions which modified the Pt electrode surface by strong adsorption at MOR potentials.

ORCID

Sanjeev Mukerjee https://orcid.org/0000-0002-2980-7655

References

1. W. Sheng, H. A. Gasteiger, and Y. Shao-Horn, "Hydrogen oxidation and evolution reaction kinetics on platinum: Acid vs alkaline electrolytes." *J. Electrochem. Soc.*, **157**, (Copyright (C) 2012 American Chemical Society (ACS). All Rights Reserved.), B1529 (2010).
2. J. R. Varcoe and R. C. T. Slade, "Prospects for Alkaline Anion-Exchange Membranes in Low Temperature Fuel Cells." *Fuel Cells*, **5**(2), 187 (2005).
3. C.-H. Chen, K. E. Meadows, A. Cuharuc, S. C. Lai, and P. R. Unwin, "High resolution mapping of oxygen reduction reaction kinetics at polycrystalline platinum electrodes." *Physical Chemistry Chemical Physics*, **16**(34), 18545 (2014).
4. E. Antolini and E. Gonzalez, "Alkaline direct alcohol fuel cells." *Journal of Power Sources*, **195**(11), 3431 (2010).
5. N. Ramaswamy and S. Mukerjee, "Influence of Inner- and Outer-Sphere Electron Transfer Mechanisms during Electrocatalysis of Oxygen Reduction in Alkaline Media." *The Journal of Physical Chemistry C*, **115**(36), 18015 (2011).
6. J. R. Varcoe, P. Atanassov, D. R. Dekel, A. M. Herring, M. A. Hickner, P. A. Kohl, A. R. Kucernak, W. E. Mustain, K. Nijmeijer, and K. Scott, "Anion-exchange membranes in electrochemical energy systems." *Energy & environmental science*, **7**(10), 3135 (2014).
7. Q. He and E. J. Cairns, "Recent progress in electrocatalysts for oxygen reduction suitable for alkaline anion exchange membrane fuel cells." *Journal of The Electrochemical Society*, **162**(14), F1504 (2015).
8. A. Bozorgnezhad, M. Shams, H. Kanani, M. Hasheminasab, and G. Ahmadi, "The experimental study of water management in the cathode channel of single-serpentine transparent proton exchange membrane fuel cell by direct visualization." *International Journal of Hydrogen Energy*, **40**(6), 2808 (2015).
9. P. Pei and H. Chen, "Main factors affecting the lifetime of Proton Exchange Membrane fuel cells in vehicle applications: A review." *Applied Energy*, **125**, 60 (2014).
10. I. Kendrick, D. Kumari, A. Yakaboski, N. Dimakis, and E. S. Smotkin, "Elucidating the Ionomer-Electrified Metal Interface." *J. Am. Chem. Soc.*, **132**(49), 17611 (2010).
11. W. Sheng, H. A. Gasteiger, and Y. Shao-Horn, "Hydrogen oxidation and evolution reaction kinetics on platinum: acid vs alkaline electrolytes." *Journal of The Electrochemical Society*, **157**(11), B1529 (2010).
12. K. C. Neyerlin, W. Gu, J. Jorne, and H. A. Gasteiger, "Study of the Exchange Current Density for the Hydrogen Oxidation and Evolution Reactions." *J. Electrochem. Soc.*, **154**, (Copyright (C) 2012 American Chemical Society (ACS). All Rights Reserved.), B631 (2007).
13. P. J. Rheinländer, J. Herranz, J. Durst, and H. A. Gasteiger, "Kinetics of the hydrogen oxidation/evolution reaction on polycrystalline platinum in alkaline electrolyte reaction order with respect to hydrogen pressure." *Journal of The Electrochemical Society*, **161**(14), F1448 (2014).
14. N. M. Marković, B. N. Grgur, and P. N. Ross, "Temperature-Dependent Hydrogen Electrochemistry on Platinum Low-Index Single-Crystal Surfaces in Acid Solutions." *The Journal of Physical Chemistry B*, **101**(27), 5405 (1997).
15. R. Notoya and A. Matsuda, "Determination of the rate of the discharge step of hydrogen ion on a hydrogen-platinum electrode in aqueous solutions by the galvanostatic transient method." *The Journal of Physical Chemistry*, **93**(14), 5521 (1989).
16. N. M. Markovic, S. T. Sarraf, H. A. Gasteiger, and P. N. Ross Jr., "Hydrogen electrochemistry on platinum low-index single-crystal surfaces in alkaline solution." *J. Chem. Soc., Faraday Trans.*, **92**, (Copyright (C) 2012 American Chemical Society (ACS). All Rights Reserved.), 3719 (1996).
17. J. H. Barber and B. E. Conway, "Structural specificity of the kinetics of the hydrogen evolution reaction on the low-index surfaces of Pt single-crystal electrodes in 0.5 M dm−3 NaOH." *Journal of Electroanalytical Chemistry*, **461**(1–2), 80 (1999).
18. J. Barber, S. Morin, and B. Conway, "Specificity of the kinetics of H2 evolution to the structure of single-crystal Pt surfaces, and the relation between opd and upd H." *Journal of Electroanalytical Chemistry*, **446**(1–2), 125 (1998).
19. E. Skulason, G. S. Karlberg, J. Rossmeisl, T. Bligaard, J. Greeley, H. Jonsson, and J. K. Norskov, "Density functional theory calculations for the hydrogen evolution reaction in an electrochemical double layer on the Pt(111) electrode." *Physical Chemistry Chemical Physics*, **9**(25), 3241 (2007).
20. A. B. Anderson, R. A. Sidik, J. Narayanasamy, and P. Shiller, "Theoretical Calculation of Activation Energies for Pt + H+(aq) + e-(U) ↔ Pt−H: Activation Energy-Based Symmetry Factors in the Marcus Normal and Inverted Regions." *The Journal of Physical Chemistry B*, **107**(19), 4618 (2003).
21. Y. Cai and A. B. Anderson, "The Reversible Hydrogen Electrode: Potential-Dependent Activation Energies over Platinum from Quantum Theory." *The Journal of Physical Chemistry B*, **108**(28), 9829 (2004).
22. E. Herrero, K. Franaszczuk, and A. Wieckowski, "Electrochemistry of Methanol at Low Index Crystal Planes of Platinum: An Integrated Voltammetric and Chronoamperometric Study." *The Journal of Physical Chemistry*, **98**(19), 5074 (1994).
23. A. V. Tripkovic, K. D. Popovic, B. N. Grgur, B. Blizanac, P. N. Ross, and N. M. Markovic, "Methanol electrooxidation on supported Pt and PtRu catalysts in acid and alkaline solutions." *Electrochimica Acta*, **47**(22–23), 3707 (2002).
24. A. V. Tripković, K. D. Popović, J. D. Momčilović, and D. M. Dražić, "Kinetic and mechanistic study of methanol oxidation on a Pt(100) surface in alkaline media." *Journal of Electroanalytical Chemistry*, **448**(2), 173 (1998).
25. J. S. Spendelow and A. Wieckowski, "Electrocatalysis of oxygen reduction and small alcohol oxidation in alkaline media." *Physical Chemistry Chemical Physics*, **9**(21), 2654 (2007).
26. T. Iwasita, "Electrocatalysis of methanol oxidation." *Electrochimica Acta*, **47**(22–23), 3663 (2002).
27. J. Jiang and A. Kucernak, "Solid polymer electrolyte membrane composite microelectrode investigations of fuel cell reactions. II: voltammetric study of methanol oxidation at the nanostructured platinum microelectrode|Nafion membrane interface." *Journal of Electroanalytical Chemistry*, **576**(2), 223 (2005).
28. J. L. Cohen, D. J. Volpe, and H. D. Abruna, "Electrochemical determination of activation energies for methanol oxidation on polycrystalline platinum in acidic and alkaline electrolytes." *Physical Chemistry Chemical Physics*, **9**(1), 49 (2007).
29. G. Yang, Y. Zhou, H.-B. Pan, C. Zhu, S. Fu, C. M. Wai, D. Du, J.-J. Zhu, and Y. Lin, "Ultrasonic-assisted synthesis of Pd–Pt/carbon nanotubes nanocomposites for enhanced electro-oxidation of ethanol and methanol in alkaline medium." *Ultrasonics sonochemistry*, **28**, 192 (2016).
30. W. Huang, H. Wang, J. Zhou, J. Wang, P. N. Duchesne, D. Muir, P. Zhang, N. Han, F. Zhao, and M. Zeng, "Highly active and durable methanol oxidation electrocatalyst based on the synergy of platinum–nickel hydroxide–graphene." *Nature communications*, **6**, 10035 (2015).
31. H. A. Gasteiger, N. M. Markovic, and P. N. Ross, "H2 and CO Electrooxidation on Well-Characterized Pt, Ru, and Pt-Ru. 1. Rotating Disk Electrode Studies of the Pure Gases Including Temperature Effects." *The Journal of Physical Chemistry*, **99**(20), 8290 (1995).
32. H. Yanagi and K. Fukuta, "Anion Exchange Membrane and Ionomer for Alkaline Membrane Fuel Cells (AMFCs)." *ECS Transactions*, **16**(2), 257 (2008).
33. T. Xu, "Ion exchange membranes: state of their development and perspective." *Journal of membrane science*, **263**(1–2), 1 (2005).
34. E. Volodina, Y. Senik, O. Basova, N. Pismenskaya, V. Nikonenko, and G. Pourcelly, "Determination of ion-exchange equilibrium coefficient for a MA-41 anion-exchange membrane in sodium carbonate/hydrocarbonate solutions." *Desalination*, **149**(1–3), 459 (2002).
35. N. Pismenskaya, E. Laktionov, V. Nikonenko, A. El Attar, B. Auclair, and G. Pourcelly, "Dependence of composition of anion-exchange membranes and their electrical conductivity on concentration of sodium salts of carbonic and phosphoric acids." *Journal of Membrane Science*, **181**(2), 185 (2001).
36. V. Nikonenko, K. Lebedev, J. A. Manzanares, and G. Pourcelly, "Modeling the transport of carbonic acid anions through anion-exchange membranes." *Electrochim. Acta*, **48**(24), 3639 (2003).
37. I. Gunasekara, M. Lee, D. Abbott, and S. Mukerjee, "Mass Transport and Oxygen Reduction Kinetics at an Anion Exchange Membrane Interface: Microelectrode Studies on Effect of Carbonate Exchange." *ECS Electrochemistry Letters*, **1**(2), F16 (2012).
38. S. Watanabe, K. Fukuta, and H. Yanagi, "Determination of carbonate ion in MEA during the alkaline membrane fuel cell (AMFC) operation." *ECS Transactions*, **33**(1), 1837 (2010).
39. C. M. Lang, K. Kim, and P. A. Kohl, "High-Energy Density, Room-Temperature Carbonate Fuel Cell." *Electrochemical and Solid-State Letters*, **9**(12), A545 (2006).
40. J. Jiang and A. Kucernak, "Investigations of fuel cell reactions at the composite microelectrode| solid polymer electrolyte interface. I. Hydrogen oxidation at the nanostructured Pt| Nafion membrane interface." *Journal of Electroanalytical Chemistry*, **567**(1), 123 (2004).
41. J. Durst, A. Siebel, C. Simon, F. Hasche, J. Herranz, and H. Gasteiger, "New insights into the electrochemical hydrogen oxidation and evolution reaction mechanism." *Energy & Environmental Science*, **7**(7), 2255 (2014).
42. C. Zalitis, J. Sharman, E. Wright, and A. Kucernak, "Properties of the hydrogen oxidation reaction on Pt/C catalysts at optimised high mass transport conditions and its relevance to the anode reaction in PEFCs and cathode reactions in electrolysers." *Electrochimica Acta*, **176**, 763 (2015).
43. L. Zhang, C. Ma, and S. Mukerjee, "Oxygen permeation studies on alternative proton exchange membranes designed for elevated temperature operation." *Electrochimica Acta*, **48**(13), 1845 (2003).
44. L. Zhang, C. Ma, and S. Mukerjee, "Oxygen reduction and transport characteristics at a platinum and alternative proton conducting membrane interface." *Journal of Electroanalytical Chemistry*, **568**(0), 273 (2004).
45. M. Ünlü, D. Abbott, N. Ramaswamy, X. Ren, S. Mukerjee, and P. A. Kohl, "Analysis of Double Layer and Adsorption Effects at the Alkaline Polymer Electrolyte-Electrode Interface." *Journal of The Electrochemical Society*, **158**(11), B1423 (2011).
46. K. Aoki and J. Osteryoung, "Diffusion-controlled current at the stationary finite disk electrode: Theory." *Journal of Electroanalytical Chemistry and Interfacial Electrochemistry*, **122**(0), 19 (1981).
47. C. P. Winlove, K. H. Parker, and R. K. C. Oxenham, "The measurement of oxygen diffusivity and concentration by chronoamperometry using microelectrodes." *Journal of Electroanalytical Chemistry and Interfacial Electrochemistry*, **170**(1–2), 293 (1984).
48. I. Gunasekara, S. Mukerjee, E. J. Plichta, M. A. Hendrickson, and K. M. Abraham, "Microelectrode Diagnostics of Lithium-Air Batteries." *Journal of The Electrochemical Society*, **161**(3), A381 (2014).
49. A. Tripković, K. D. Popović, J. Momčilović, and D. Draić, "Kinetic and mechanistic study of methanol oxidation on a Pt (111) surface in alkaline media." *Journal of Electroanalytical Chemistry*, **418**(1), 9 (1996).

50. Y. M. Tsou, M. C. Kimble, and R. E. White, "Hydrogen Diffusion, Solubility, and Water Uptake in Dow's Short-Side-Chain Perfluorocarbon Membranes." *Journal of The Electrochemical Society*, **139**(7), 1913 (1992).
51. Z. Ogumi, Z. Takehara, and S. Yoshizawa, "Gas Permeation in SPE Method." *Journal of The Electrochemical Society*, **131**(4), 769 (1984).
52. L. Chaabane, G. Bulvestre, C. Innocent, G. Pourcelly, and B. Auclair, "Physico-chemical characterization of ion-exchange membranes in water–methanol mixtures." *European Polymer Journal*, **42**(6), 1403 (2006).
53. E. Skou, P. Kauranen, and J. Hentschel, "Water and methanol uptake in proton conducting Nafion membranes." *Solid State Ionics*, **97**(1–4), 333 (1997).